TUDelft

Delft University of Technology

The Investigation of Archaeological Glass Using X-Ray Fluorescence Spectroscopy and X-Ray Micro Computed Tomography

Verhaar, G.; van Eijck, L.; Ngan-Tillard, D.J.M.; van Beek, Rene; Megens, Luc

Important note
To cite this publication, please use the final published version (if applicable).
Please check the document version above.

The Investigation of Archaeological Glass Using X-Ray Fluorescence Spectroscopy and X-Ray Micro Computed Tomography

ABSTRACT

X-ray fluorescence spectroscopy (XRF) and X-ray micro computed tomography (µ-CT) were applied to the study of four archaeological glass objects from the collection of the Allard Pierson in Amsterdam, The Netherlands. Often, little is known about the provenience and provenance of archaeological glass objects, as documentation is regularly insufficient to assign a specific place and date of excavation or place of production. This paper demonstrates the value of µ-CT for visualising the internal structures of archaeological glass objects, providing insight into production techniques and condition. The XRF results presented are consistent with published glass compositions but are, as yet, insufficient to assign the glass objects to a specific place of production. Part of a broader research project to apply non-destructive techniques to the study of archaeological glass objects, the results presented here will be the basis for the future evaluation of less commonly applied methods, such as neutron tomography and gamma spectroscopy.

KEYWORDS

Archaeological glass • Provenance • Glass composition • X-ray fluorescence spectroscopy • Micro computed tomography • Production techniques

AUTHORS

Guus Verhaar*
Postdoctoral Researcher, Delft University of Technology, Faculty of Applied Sciences, Department of Radiation Science and Technology, Neutron and Positron Methods for Materials, Delft, The Netherlands
g.verhaar@tudelft.nl

Lambert van Eijck
Assistant Professor, Delft University of Technology, Faculty of Applied Sciences, Department of Radiation Science and Technology, Neutron and Positron Methods for Materials, Delft, The Netherlands
l.vaneijck@tudelft.nl

Dominique Ngan-Tillard
Assistant Professor, Delft University of Technology, Faculty of Civil Engineering and Geosciences, Department of Geoscience and Engineering, Delft, The Netherlands
d.j.m.ngan-tillard@tudelft.nl

René van Beek
Curator Classical World, Allard Pierson, Collections of the University of Amsterdam, Department of Knowledge and Collections, Amsterdam, The Netherlands
r.vanbeek@uva.nl

Luc Megens
Senior Heritage Scientist, Cultural Heritage Agency of the Netherlands, Heritage Materials Laboratory, Amsterdam, The Netherlands
l.megens@cultureelerfgoed.nl

*Corresponding Author

INTRODUCTION

The Allard Pierson (AP) holds and exhibits the heritage collections of the University of Amsterdam, including a significant collection of archaeological glass. The collection encompasses glassmaking ranging from very early glass produced in Mesopotamia, dated ca. 14th century BCE, to Egyptian and Syrian glass objects from late antiquity, dated ca. 9th–12th century CE. The University acquired most of these objects through donations, bequests, and the art trade (Van Beek 2021), lacking documentation about their archaeological origins, or provenience. This was

particularly evident in a group of objects referred to as the 'Palmyra collection': 43 pieces all allegedly acquired in Palmyra, Syria, according to the Museum's records. The objects are catalogued with dates ranging from ca. 50 CE to 1150 CE, but they were sold to the Museum in the 1950s without any supporting documentation as to their origins.

Determining the provenance of archaeological glass objects is a challenge in the field of archaeometry, as characteristics of the raw materials used, such as crystal structure and grain size, are lost during

glass production. Therefore, typical methods to attribute glass to a specific production place rely on determining the elemental composition of the bulk glass and the analysis of isotope ratios of trace elements, specifically strontium (Sr) and neodymium (Nd). For example, the amount of strontium and its isotope ratio of $^{87}Sr/^{86}Sr$ may provide information on whether the lime used originates from marine environments, such as limestone or shell-baring coastal sands, or from plant ash (Freestone et al. 2006). Typical means of analysis include inductively coupled plasma-mass spectrometry (ICP-MS), thermal ionisation mass spectrometry (TIMS), and X-ray microprobe analysis in an electron microscope (Freestone et al. 2006; Degryse and Shortland 2009; Wedepohl, Simon, and Kronz 2011; Ganio 2013). These techniques require extensive, invasive, and destructive sample preparation, such as ablation of a small part of the sample, polishing the glass down to the bulk material, or cleaning the glass using acidic solutions, limiting the study of intact objects. Therefore, research into archaeological glass has primarily utilised shards, glass waste, and study objects, or has required accepting local damage to an object to remove a small sample.

Typologies, such as the one developed by Isings (1957), constitute indispensable tools to classify and date archaeological glass, but the definitive attribution to a production site remains difficult. Importantly, the origin of glass as a raw material and the origin of a glass object are not necessarily the same, which relates to different theories concerning glass production in antiquity. The centralised production model posits raw glass production in a small number of large-scale production centres, while the dispersed production model suggests a larger number of small glass-production centres (Ganio 2013).

A research project initiated by the AP and Delft University of Technology aims to develop new methodologies for the non-destructive study of archaeological glass and compare them to existing methods of study, focussing on the application of four techniques: X-ray fluorescence spectroscopy (XRF), X-ray micro computed tomography (μ-CT), neutron tomography, and gamma spectroscopy.

Driving the development of these methods, three research questions emerged during the study of the Palmyra collection:

- Can a relationship between glass composition and origin be established?
- Can the objects' production techniques be elucidated?
- Can the condition of the glass, including the identification of damages, restorations, weathering, or iridescent layers, be described?

This paper describes the application of XRF and μ-CT to four objects from the AP collection, comprising the first results of the project and providing a comparative basis for the future application of less commonly applied techniques, such as neutron tomography and gamma spectroscopy.

METHODS

Objects

Four objects from the AP collection were selected for this study: three bottles from the Palmyra collection and an Iranian glass rod (Figure 1). The Museum's inventory cards describe the bottles (Figures 1a–c) as originating from Palmyra; however, the authors know of no archaeological evidence of large-scale glass production there. Conversely, the rod formed part of an architectural decoration found in Chogha Zanbill, an impressive excavation site in Iran, and is dated ca. 1250 BCE. All three bottles are free blown and represent different periods and decorative techniques, allowing us to investigate the potential of the analytical methods on varied objects.

Object 504 (Figure 1a) is a black glass bottle decorated with red glass trailed and then worked into a zig-zag pattern. The vessel is cracked, with losses to one side and the rim. Object 1110 (Figure 1b) is a *balsamarium*, a cosmetic flask or container for scented oil, made of green glass and decorated with handles and a trail wound around the body. It is partially covered with an opaque layer, a particular degradation pattern, and its foot is a restoration. Object 1154 (Figure 1c) is a double-bodied *balsamarium*, comprising two conjoined tubular phials separated by a diaphragm, which

Figure 1. Four objects from the Allard Pierson collection: a) Palmyra, Syria (?), Black and red bottle, ca. 650–750 CE, glass, H 77 mm × Diam. 25 mm. Allard Pierson, 504; b) Palmyra, Syria (?), Bottle, ca. 300–400 CE, glass, H 100 mm × W 28 mm. Allard Pierson, 1110; c) Palmyra, Syria (?), Double-bodied *balsamarium* (*Kohl* tube), ca. 4th century CE, glass, H 107 × W 26 mm. Allard Pierson, 1154; and d) Chogha Zanbil, Iran, Rod, ca. 1250 BCE, glass, H 44 mm × Diam. 14 mm. Allard Pierson, 9377

is created by pinching the glass on opposing sides (Whitehouse 2001, No. 722–751). Vessels like this were also used to store galena, or black lead sulphide, for use as eye makeup, in which case they are referred to as *kohl* bottles (Sultan and Khasawneh 2015). Object 9377 (Figure 1d) is a fragment of a core-formed, blue and white glass rod with spiral decoration.

XRF

XRF analysis was performed using a Bruker ARTAX micro-XRF spectrometer equipped with an X-ray tube containing a molybdenum anode and operated at a voltage of 50 kV and an applied current of 600 µA. The X-ray beam was focussed on the sample by a poly-capillary lens with a spot size of 0.065 mm. The space between the detector and the sample surface was flushed with helium to increase sensitivity for light elements. Spectra were collected on clean areas of the glass, with at least three measurements for each glass colour. Spectra were analysed with PyMCA software (Solé et al. 2007) to obtain peak intensities for the detected elements. No quantitative data was obtained, but the peak areas were compared to evaluate detected elements' relative amounts.

X-ray µ-CT

X-ray µ-CT allows for the non-destructive investigation of the three-dimensional (3D) characteristics and internal structures of a wide range of samples, including archaeological artefacts (Tuniz and Zanini 2018). During scanning, X-rays pass through the object, are variably attenuated, and hit a detector that produces a two-dimensional greyscale image. Variations in elemental composition or material density will cause differences in X-ray attenuation. In the resulting image, the grey value represents the extent of X-ray attenuation: the more the X-rays are attenuated, the lighter the colour. For µ-CT, a series of X-ray projections is collected by rotating the sample in the X-ray beam and recording an image at each rotation step. These images are then used to reconstruct a 3D model of the object. Subsequently, this reconstruction can be used to create virtual cross sections through the object at any location and in any direction, revealing the object's internal structure (Cantatore and Müller 2011; Cnudde and Boone 2013).

Each object was wrapped in acid-free paper and bubble wrap and placed inside a paper cup to immobilise it for scanning. These materials were chosen as they cause minimal X-ray attenuation. Scans were obtained using a benchtop Phoenix

X-ray Nanotom μ-CT scanner at a lateral resolution of 30 μm. Two-dimensional X-ray images were acquired for each object on a flat panel CCD detector by rotating the object 360 ° with a rotation step of 0.25 °, resulting in a total of 1440 X-ray projection images saved as 16-bit tiff files with grey values ranging from 0 to 65536. Five images were captured at each rotation step, the average of the last four of which was calculated using the numerical value of the grey hue of each pixel. These average images were used to compute the 3D reconstruction, modelled with StudioMax 2.0 software. The 3D model was then processed using Avizo 9.4 software and visually examined to interpret the results of μ-CT.

For μ-CT scanning, data processing requires correction of artefacts, including beam hardening: if the X-rays passing through the sample are not monochromatic, lower energy photons are selectively attenuated, resulting in a higher mean beam energy. If not corrected, this results in images that suggest high attenuation along the circumference of the sample as imaged. This is because the pathlength of X-rays passing through the sides of the object — where the tangent to the object's surface is parallel to the X-ray beam direction — is longer than that of X-rays passing through the front and back of the object relative to the origin of the beam, where the tangent to the object's surface is perpendicular to the beam direction. For each object imaged in this study, a beam hardening correction was iteratively applied to a zone expected to consist of homogeneous glass, identified based on the first reconstruction, until the area presented homogeneous X-ray attenuation in the resulting projections. With only one correction parameter, it is difficult to correct properly the beam hardening for heterogeneous objects having a non-regular cylindrical section. Ngan-Tillard et al. (2018) provide detailed information on μ-CT scanning equipment and methodology, including parameters for beam-hardening corrections during data processing.

RESULTS AND DISCUSSION

Provenance determination through compositional analysis

Compositional data provides the most information about the provenance of a glass object. Extensive study has identified the general composition of Roman glass as soda-lime glass containing silicon (Si), sodium (Na), calcium (Ca), iron (Fe), and manganese (Mn) (Sayre and Smith 1961).

XRF analysis of object 504 (Figure 1a) indicates a base glass composition consisting of silicon, calcium, potassium (K), and iron. The red glass contains copper (Cu) and more lead (Pb) as compared to the black glass, consistent with published data on ancient red glass (Barber, Freestone, and Moulding 2009). No additional colourants were identified for the black glass. This is also consistent with the literature, as ancient black glass typically comprises a very dark hue of another colour, such as green or purple made with iron (II) oxide or manganese oxide, respectively (Van der Linden et al. 2009). Compared to unpublished analyses of earlier glass objects from the Palmyra collection, substantially more potassium was detected in both colours and particularly in the red glass, which is not unusual for glass dated after 600 CE and indicates the use of plant ash instead of natron as a flux (Rosenow and Rehren 2018). Additionally, a relatively low amount of strontium (Sr) was detected, relating to the source of calcium, potentially limestone (Freestone et al. 2006). Unfortunately, XRF analysis cannot further elucidate the source of the lime, but additional research could clarify this.

The base glass of object 1110 (Figure 1b) consists of silicon, calcium, manganese, and iron, with significantly more calcium in the translucent green glass and with more manganese in the opaque weathering layer. These observations are consistent with previous studies that mention manganese-rich inclusions in the degradation layers of archaeological glass due to burial conditions (Schalm and Anaf 2016).

XRF analysis of object 1154 (Figure 1c) indicates a composition rich in silicon, calcium, iron, and

manganese, with a small amount of potassium, typical for Roman glass.

Object 9377 (Figure 1d) comprises silicon, potassium, calcium, and iron. Unexpectedly, no copper or cobalt (Co) was detected in the blue glass, but iron and sulfur (S) were. Schreurs and Brill (1984) have reported that iron in combination with sulfur may cause glass to appear blue. Similarly, no antimony (Sb), the most common white colourant and opacifier for glass (Dillis et al. 2019), was found in the white glass.

Production techniques

The µ-CT data provides information on production techniques, including forming and the application of decorative elements.

For object 504, differences in attenuation between the copper-rich red glass and the black glass allow for a segmentation of the different colours, demonstrating that the red glass was applied to the black glass bottle as a thin trail that was then manipulated to achieve the final decorative pattern (Figure 2).

The modern addition of a wax support at the base of object 1110 is clearly differentiable in the µ-CT scan (Figure 3, location 1); bottles of this type usually have a different-shaped foot or no foot at all (Arveiller-Dulong and Nenna 2005, 412–413). Interestingly, the µ-CT cross sections and reconstruction do show a curvature near the base of the vessel's walls (Figure 3, locations 3), suggesting some form of finishing. Whether or not this was part of a foot remains unclear.

The µ-CT scans of object 1154 (Figures 4 and 5) provide insights into how the double-bodied vessel was created. The diaphragm between the phials is of uneven thickness, with more glass at its centre and a void running its entire length. This suggests that the diaphragm was created by pinching a single, wide tube along its length and subsequently pressing the sides towards each other to create a closed diaphragm, trapping some air in between the previously exterior walls. The uneven thickness of the diaphragm results from unequal pressure on both sides as the form is pinched. Additionally, each handle was fixed to the vessel as a small bit of glass,

Figure 2. 3D reconstruction created from X-ray µ-CT scans of object 504, with false colours indicating the different X-ray attenuations of the black glass (orange), the red glass (yellow), and restoration material (green)
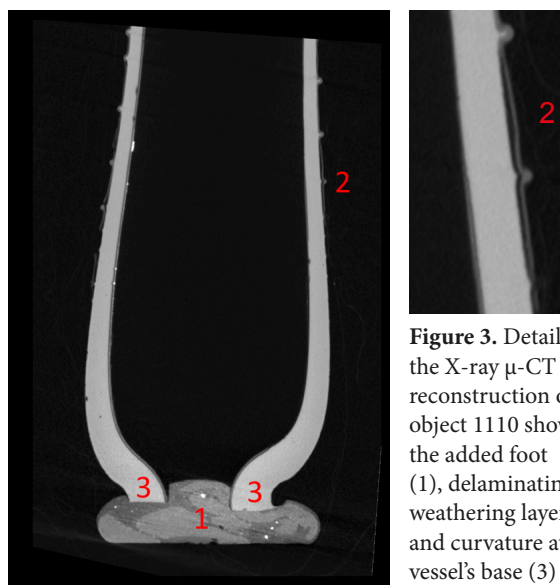

Figure 3. Detail of the X-ray µ-CT 3D reconstruction of object 1110 showing the added foot (1), delaminating weathering layers (2), and curvature at the vessel's base (3)

Figure 4. Horizontal X-ray µ-CT cross section of object 1154 showing the handles at the vessel's sides, the diaphragm, and the onset of the decorative glass trail at the bottom of the image
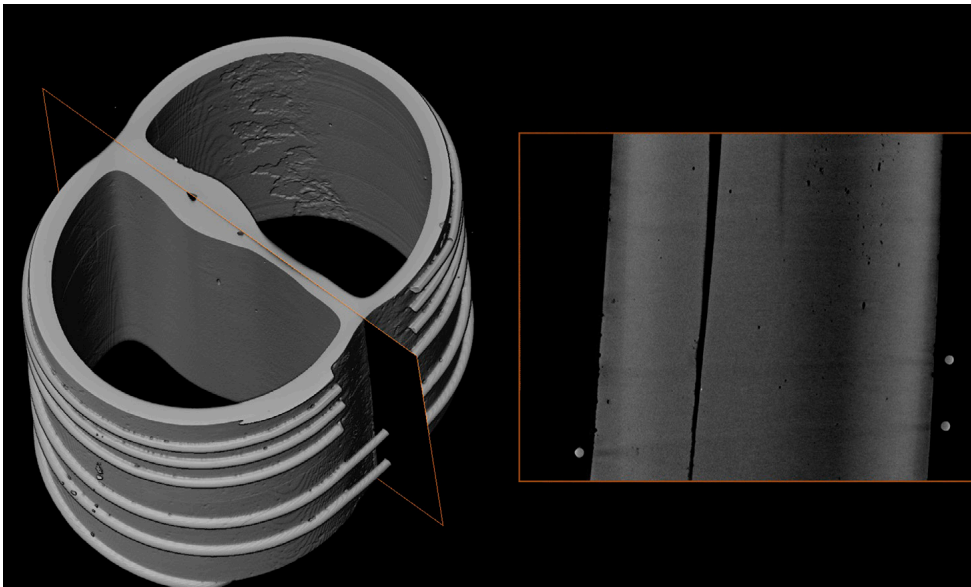
Figure 5. Section of the 3D reconstruction (left) and the highlighted cross section (right) of object 1154

which was then pulled up and terminated against the side of the bottle. The onset of the thin glass trail wrapped around the object is visible in Figure 4; this trail has since suffered losses in some places where it was not in contact with the bottle (Figure 5).

The μ-CT cross section of object 9377 clearly shows more bubbles in the white glass than in the blue (Figure 6). With some large bubbles that appear to have stretched, the blue glass was probably formed by winding molten glass around a cylindrical core, most likely made of copper (Emami et al. 2020). The white glass forms a wide spiral decoration that has completely sunken into the blue glass and is flush with the surface of the rod. Given the absence of antimony, the diffusion of light by the preponderance of bubbles may be causing the material to appear white. Emami et al. (2020) identified the presence of crystalline phases, calcite, gehlenite, quartz, and argentojarosite, in similar glass rods; the opacity of the object may also relate to their presence. Because these minerals consist of calcium, silicon, and iron — the same elements as the glass phase — non-invasive elemental analysis alone is not very helpful. Conversely, argentojarosite contains silver (Ag), which would be distinguishing but was not detected with XRF.

Condition

X-ray μ-CT scanning can elucidate condition as it allows for segmentation of different parts of
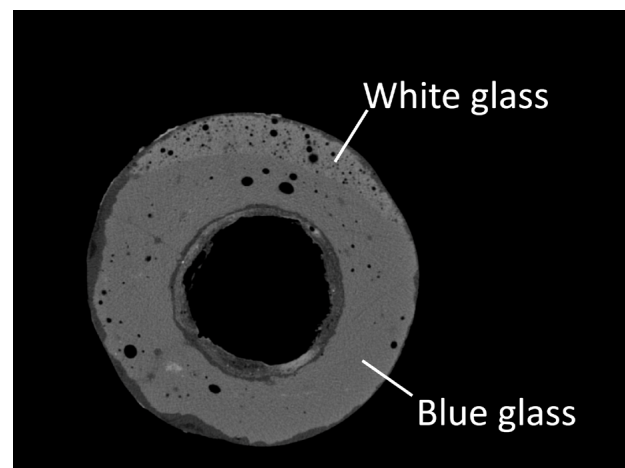

Figure 6. Horizontal X-ray μ-CT cross section of object 9377 showing more air bubbles in the white glass as compared to the blue glass

an object based on density. Generally of lower density, restorations and degradation layers become distinguishable from intact glass. XRF analysis may provide information on the materials used for restoration or on changes in glass composition as a result of degradation.

The μ-CT scan of bottle 504 (Figure 2) reveals the presence and extent of a restoration, including a drip of the low-attenuating restoration material on the vessel's interior. The μ-CT scan also shows cracks, invisible to the unaided eye, throughout the object, some of which extend through the entire thickness of the wall, demonstrating the object's fragile condition.
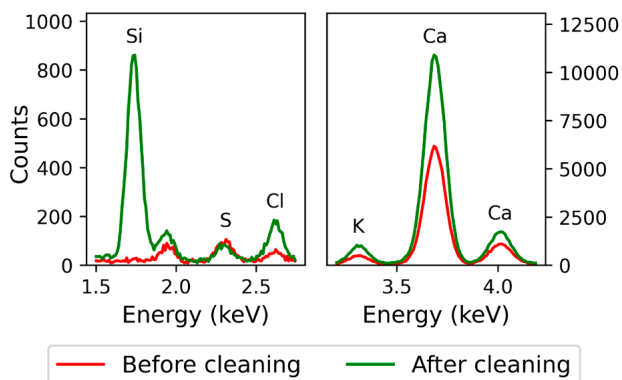
Figure 7. Partial XRF spectra of two measurements conducted on the same location on object 1110, one before (red) and one after (green) cleaning the area with acetone. Cleaning resulted in improved detection of silicon, chlorine, potassium, and calcium.

The scans of object 1110 reveal a sharp boundary between the weathering layers and the bulk glass, which appears homogeneous (Figure 3, location 2). Visualising the delamination of the weathering layers can help identify areas at risk of material loss. In some areas, no silicon was initially detected with XRF. After cleaning with acetone, subsequent XRF analysis in the test area did result in the detection of silicon, as well as improved signals for chlorine (Cl), potassium, and calcium (Figure 7). In the archaeological glass trade in the 20th century, objects were often coated overall, including with commonly available materials like hairspray, to consolidate loose material. These coatings can create confusing XRF results, as the fluorescent X-rays characteristically originating from silicon, chlorine, potassium, and calcium are of such low energies that they are attenuated by the coating material itself and do not reach the detector. The suspected consolidant layer on object 1110 was not visible on the µ-CT scans, likely because the layer thickness is close to the scanning resolution of the instrument and the X-ray energy is too high for any noticeable attenuation.

Future perspectives

The study of these four glass objects will continue with neutron tomography, another imaging technique complementary to X-ray µ-CT, and gamma spectroscopy. Because neutrons interact with the nucleus of an atom, where they are absorbed or scattered resulting in neutron attenuation, and X-rays interact with electrons

surrounding the core, the two tomographic techniques are sensitive to different elements. Combining these tomographies can produce a set of attenuation images representing nearly every element on the periodic table. During neutron tomography, exposure to neutron radiation will cause the glass constituents to become slightly radioactive, enabling characterisation of the glass composition by neutron activation analysis (NAA) through gamma spectroscopy. Unlike XRF, gamma spectroscopy will provide information on the bulk glass composition, as the penetration depths of neutrons and gamma rays are much greater than the thickness of the glass. This data can be compared with XRF results to improve our understanding of XRF analysis of archaeological glass. For instance, the XRF instrument cannot detect sodium because the characteristic X-rays will be absorbed in the helium-flushed air between the sample and the detector. Additionally, because of absorption of low-energy fluorescent X-rays in the sample itself, sodium would only be detectable from the top few micrometres of the sample; and, for archaeological glass, this surface layer is often depleted in sodium. Future NAA of the objects will provide a quantitative measure of the sodium content, which will aid efforts to determine the origin of the glass.

Because neutron tomography renders the object temporarily radioactive, an object is returned to its owner only after clearance by an independent radioprotection authority in accordance with the national nuclear regulations of The Netherlands, usually within several hours, days, or weeks following exposure.

Expanding the scope of this research, the National Museum of Antiquities in Leiden has agreed to provide access to their collection of ancient glass, so that the authors may study reference objects with well-documented provenance in the Eastern Mediterranean and compare these objects to those of the Palmyra collection.

CONCLUSIONS

This paper outlines the first results of a research project to develop a suite of non-destructive analytical techniques for the study of archaeological

glass objects, specifically those with unknown provenance and provenience. The present study focussed on obtaining compositional information for four archaeological glass objects using XRF and on visualising their structures using μ-CT.

The results obtained thus far with XRF, a commonly applied technique, are consistent with existing literature but are insufficient to attribute the glass to specific production centres. Quantification of glass composition with XRF and interpretation of XRF data, especially for archaeological glass with weathering layers, remains difficult. Non-original coatings or consolidants may cause unreliable results, as demonstrated for object 1110.

X-ray μ-CT allows for visualisation of the internal structure of vessels, providing insight into production techniques and object condition. The high spatial resolution of μ-CT scans helps contextualise the results of other techniques, such as XRF, for which data can be cross referenced with the object's actual structure in order to better understand its physicochemical nature.

The combination of techniques is promising for understanding glass condition, manufacture, and provenance. Ultimately, we hope an accurate analysis by non-destructive means will provide insight into the origins of the glass objects studied here. In future work, glass with a known archaeological context will serve as a comparison for glass without archaeological provenance.

ACKNOWLEDGEMENTS

REFERENCES

Arveiller-Dulong, V., and M.-D. Nenna. 2005. *Les verres antiques du Musée du Louvre*. Vol. 2. Paris: Somogy.

Barber, D. J., I. Freestone, and K. M. Moulding. 2009. Ancient copper red glasses: Investigation and analysis by microbeam techniques. In *From mine to microscope: Advances in the study of ancient technology*, eds. A. J. Shortland, I. C. Freestone, and T. Rehren, 117–128. Oxford: Oxbow Books.

Cantatore, A., and P. Müller. 2011. *Introduction to computed tomography*. Kongens Lyngby: DTU Mechanical Engineering. https://orbit.dtu.dk/en/publications/introduction-to-computed-tomography.

Cnudde, V., and M. N. Boone. 2013. High-resolution X-ray computed tomography in geosciences: A review of the current technology and applications. *Earth-Science Reviews* 123: 1–17.

Degryse, P., and A. J. Shortland. 2009. Trace elements in provenancing raw materials for Roman glass production. *Geologica Belgica* 12(3): 135–143.

Dillis, S., A. van Ham-Meert, P. Leeming, A. Shortland, G. Gobejishvili, M. Abramishvili, and P. Degryse. 2019. Antimony as a raw material in ancient metal and glass making: provenancing Georgian LBA metallic Sb by isotope analysis. *STAR: Science & Technology of Archaeological Research* 5(2): 98–112.

Emami, M., A. S. H. Rozatian, O. Vallcorba, M. Anghelone, M. H. Dehkordi, C. Pritzel, and R. Trettin. 2020. Synchrotron micro-XRD study, the way toward a deeper characterizing the early prehistoric Iranian glass cylinders from Late Bronze Age (1280 BC). *The European Physical Journal Plus* 135(6): art. 487.

Freestone, I. C. 2006. Glass production in Late Antiquity and the Early Islamic period: A geochemical perspective. In *Geomaterials in cultural heritage, Geological Society London Special Publications* 257(1), eds. M. Magetti and B. Messiga, 201–216. London: Geological Society London.

Ganio, M. 2013. A 'true' Roman glass. Evidence for primary production in Italy. Ph.D. dissertation, Katholieke Universiteit Leuven, Belgium.

Isings, C. 1957. *Roman glass from dated finds*. Groningen and Djakarta: J. B. Wolters.

Ngan-Tillard, D. J. M., D. J. Huisman, F. Corbella, and A. van Nass. 2018. Over the rainbow? Micro-CT scanning to non-destructively study Roman and Early Medieval glass bead manufacture. *Journal of Archaeological Science* 98: 7–21.

Rosenow, D., and T. Rehren. 2018. A view from the South: Roman and Late Antique glass from Armant, Upper Egypt. In *Things that travelled: Mediterranean glass in the first millennium AD*, eds. D. Rosenow, M. Phelps, A. Meek, and I. C. Freestone, 283–323. London: UCL Press.

Sayre, E. V., and R. W. Smith. 1961. Compositional categories of ancient glass. *Science* 133(3467): 1824–1826.

Schalm, O., and W. Anaf. 2016. Laminated altered layers in historical glass: Density variations of silica nanoparticle random packings as explanation for the observed lamellae. *Journal of Non-Crystalline Solids* 442: 1–16.

Schreurs, J. W. H., and R. H. Brill. 1984. Iron and sulfur related colors in ancient glasses. *Archaeometry* 26(2): 199–209.

Solé, V. A., E. Papillon, M. Cotte, P. Walter, and J. Susini. 2007. A multiplatform code for the analysis of energy-dispersive X-ray fluorescence spectra. *Spectrochimica Acta Part B: Atomic Spectroscopy* 62(1): 63–68.

Sultan, Z., and A. Khasawneh. 2015. Facial beauty: A collection of glass Kohl containers from the north of Jordan. *Mediterranean Archaeology and Archaeometry* 15(1): 83–93.

Tuniz, C., and F. Zanini. 2018. Microcomputerized tomography (MicroCT) in archaeology. In *Encyclopedia of global archaeology*, ed. C. Smith, 1–7. Cham: Springer International Publishing.

Van Beek, R. 2021. Antiek glas in het vernieuwde Allard Pierson. *Vormen uit Vuur* 245: 20–25.

Van der Linden, V., P. Cosyns, O. Schalm, S. Cagno, K. Nys, K. Janssens, A. Nowak, B. Wagner, and E. Bulska. 2009. Deeply coloured and black glass in the northern provinces of the Roman empire: Differences and similarities in chemical composition before and after AD 150. *Archaeometry* 51(5): 822–844.

Wedepohl, K. H., K. Simon, and A. Kronz. 2011. The chemical composition including the rare earth elements of the three major glass types of Europe and the Orient used in Late Antiquity and the Middle Ages. *Geochemistry* 71(3): 289–296.

Whitehouse, D. 2001. *Roman glass in the Corning Museum of Glass*. Vol. 2, Hudson Hills Press: New York.